Redoximorphic Macropore Environments in an Agrudalf

Lars Holm Rasmussen[1], Vibeke Ernstsen[2] and Hans Christian Bruun Hansen[1]

[1]Royal Vet. and Agri. Univ., DK-1871 Frederiksberg C, Denmark
[2]Geological Survey of Denmark, DK-2400, Copenhagen

Soil materials in fracture walls may strongly interact with solutes and colloidal particles during preferential flow. Wall coatings rich in metal oxides, clays, and organic matter may increase sorption capacities, whereas coatings devoid of these constituents have the opposite effect of increasing the risk of leaching of otherwise strongly sorbing solutes. The contrasting compositions between bulk horizon and fracture wall materials of a Typic Agrudalf excavated at Flakke-bjerg, Denmark, were studied by using chemical and micromorphological methods. In the upper 220 cm of the profile, the predominant desiccation and shear fractures had 2-30 mm thick hypocoatings depleted of Fe-oxides with adjacent 5-20 mm thick quasi-coatings containing 5-6 times as much Fe-oxide. Thin hypocoatings covering walls of smaller voids and surfaces of sand particles and with strong enrichments of Fe- and Mn-oxides occurred throughout the profile, but were most abundant below 220 cm. Fracture walls, commonly with distinct laminas of clay, silt, and organic matter, generally had slightly coarser texture, but were enriched in smectite compared with horizon materials. Higher contents of organic C in fracture coatings were attributed to root growth and deposition of A-horizon materials. Despite removal of Fe-oxides from depletion hypocoatings, no corresponding depletion of P was observed. However, calculations demonstrated that, in the case of macropore transport only, P sorption capacity would be at least 5 times less than during piston-like matrix flow. For adequate estimations of solute leaching from macroporous soils there is a strong need to properly take into account sorption properties of macropore wall materials!

333

Introduction

For many years it has been the assumption that loamy glacial deposits can act as an effective filter of anthropogenic pollutants to the groundwater. However, during the last ten years an increasing number of pollutants have been found in the groundwater below these kinds of glacial deposits (Keller *et al.* 1988; Jørgensen and Fredericia 1992; Jørgensen *et al.* 1993; McKay *et al.* 1993). It is now recognized that clayey tills contain preferential and fast-conducting flow paths, such as sandy inhomogeneities and well-developed fracture systems. The fracture systems have developed during glaciations and in postglacial time, whereas the sandy inhomogeneities are depositional irregularities (Jørgensen and Fredericia 1992; McKay *et al.* 1993).

Different kinds of fracture systems can be distinguished based on their origin. Typically 3 or 4 different fracture systems may be present in the till units, which include: i) shear fractures; ii) extensional fractures; iii) relief fractures; and iv) non-systematic fractures. Shear, extensional, and relief fractures are systematic fractures with pronounced horizontal or vertical orientations formed by glacio-tectonic forces down to approximately 10 metres (Klint and Fredericia 1995; McKay and Fredericia 1995). Non-systematic geophysical fractures are formed in the upper 2 to 3 metres of the till as the result of freeze-thaw processes and/or as the result of contraction due to desiccation. Non-systematic macropores of biological origin evolve in the upper 1 to 2 metres of soil. The different kinds of macropores are interconnected resulting in a continuous pore system throughout the till (Jensen 1998). When the amount and intensity of precipitation exceeds the infiltration capacity of the soil, conditions for bypass flow are established. This flow pattern can occur both during saturated and unsaturated soil conditions. When bypass flow occurs, solutes including pollutants, can be rapidly transported over long distances within the soil (Beven and Germann 1982; Andreini and Steenhuis 1990; Jardine *et al.* 1990; Vepraskas *et al.* 1991).

The geochemical environment around macropores may differ strongly from that in the soil matrix. For example, pseudogley properties are observed in the upper 2 to 3 m of clayey sediments, as indicated by depletion hypocoatings next to macropores and the formation of Fe-oxide-hydroxide quasi-coatings at a distance of 1-10 mm inside the soil matrix (Bullock *et al.* 1985; Jørgensen and Fredericia 1992; McKay and Fredericia 1995; Vepraskas and Wilding 1983; Vepraskas *et al.* 1994). In addition, ferrolysis caused by shifting redox conditions in the soil tends to lower the pH in the macropore environment (Brinkmann 1970). Below this zone Fe- and Mn-oxide-hydroxide hypocoatings may be present as fracture coatings (McKay and Fredericia 1995; Vepraskas *et al.* 1994). In earthworm burrows and other kinds of voids in the upper 2 metres, organic matter commonly covers the void walls (Jensen 1998). Clay and silt coatings are commonly observed in some of the fractures and biopores in the upper 1 to 2 m due to argillization (Khalifa and Buol 1968). The microbiological activity in the macropores is higher than in the soil matrix, demonstrating that macro-

pores are the preferential environment for microbial degradation of organic matter and other microbial processes (Vinther *et al.* 1999). These findings demonstrate that soil properties determined for bulk horizons do not represent the environment that preferentially moving water encounters on its way through the till.

The aim of this study was to describe, characterize and quantify redoximorphic environments around geophysically induced fractures and biologically formed macropores in a clayey till. The study demonstrates the need for micro-pedological and environmental investigations to quantify the actual soil environments that percolating water interacts with.

Materials and Methods

Site Conditions

The study site is located on a typical, almost flat, glacial plain at Flakkebjerg, Denmark (Fig. 1). The parent material was deposited during the Weichsel-glaciation and the age of the top-till is estimated to be 13-15,000 years (Kronborg 1995; Klint and Gravesen 1999). The soil moisture regime is udic and the soil temperature regime is mesic (Soil Survey Staff 1994; Tiberg 1998). The site has been used for agricultural purposes for centuries.

Field Methods

Three profiles were excavated at the site, however, because the profiles were very similar, only one is described in the following. The Flakkebjerg profile was excavated to a depth of approximately 500 cm, with the horizontal dimensions of 650×400 cm. In this pit a standard soil profile representative for the area was described and classified following FAO (1990) and Soil Survey Staff (1994) procedures. Soil samples were collected from all horizons (bulk-horizons) and from parts of adjacent hypo- and quasi-coatings along three fractures, comprising: 1) a vertical desiccation fracture (50-130 cm), 2) a subvertical shear fracture following the border between layers of clayey and sandy meltwater deposits (160-180 cm), and 3) a small vertical fracture of unknown origin (180-190 cm). Approximately 50 grams of soil were sampled from each type of coating.

Undisturbed samples for preparation of thin sections were collected from all horizons and from the fracture zones using Kubiena-boxes (3×5×10 cm) according to Murphy (1986) and FitzPatrick (1993).

Laboratory Methods

The soil samples were air dried, gently crushed and sieved through a 2 mm screen. Particle size distribution in the bulk-horizons was measured using the hydrometer method (Bouyoucos 1926). Because of lack of soil-material, the particle size distribution of the hypocoatings was measured gravimetrically after sieving and centrifu-
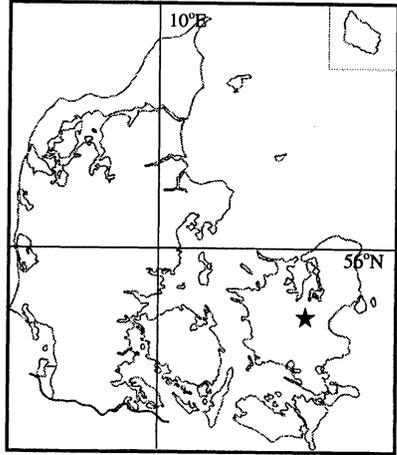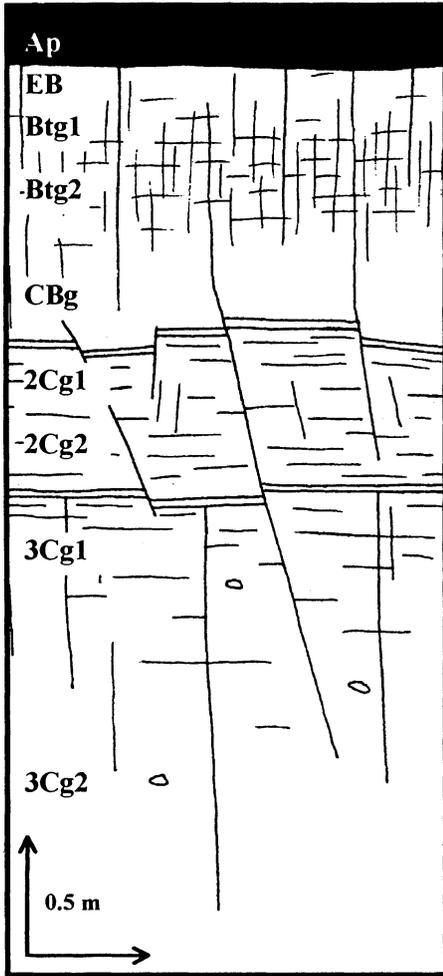
Map of Denmark with the location of Flakkebjerg.
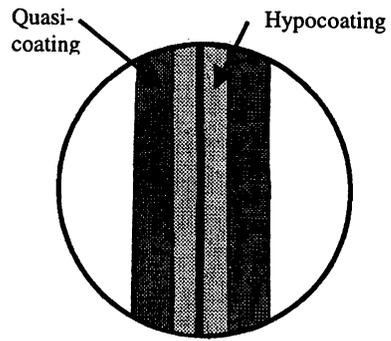
Void wall characters in the upper 2 metres.

Fig. 1. Location and geological setting at the Flakkebjerg site. The profile consists of three lithological units (approximate depths): i) 0-1.5 m, lodgement-till, ii) 1.5-2.2 m, melt-water deposits, iii) 2.2-12 m: lodgement-till. The profile contains several fracture systems as shown in the figure. Void wall characteristics in the upper 2 m (hypocoatings and quasi-coatings) are shown to the right (not to scale).

gation. The content of calcite was measured gas-volumetrically (Collins 1906). Organic carbon was determined by dry combustion using an Eltra CS 500 Carbon Sulfur Determinator (Nelson and Sommers 1986). Soil pH was measured in a 0.01 M calcium chloride suspension (1:2.5 soil:liquid). Ammonium oxalate extractable iron (oxide) hydroxides (Fe_o) and aluminium (oxide) hydroxides (Al_o) were extracted according to Schwertmann (1964). Citrate-bicarbonate-dithionite extractable iron

336

oxides (Fe_d) and aluminium (oxide) hydroxides (Al_d) were extracted according to Mehra and Jackson (1960). The total content of phosphorous was extracted with 6 M sulphuric acid after ignition of the sample at 550°C (Mehta *et al.* 1954). Phosphorus in the citrate-bicarbonate-dithionite solutions (P_d) was determined after acid oxidation of the samples with concentrated nitric acid (Westergaard and Hansen 1997). All measurements were made in duplicate.

The soil samples were fractionated into the following particle-size classes after treatment with sodium pyrophosphate: Sand (20-2000 µm), silt (2-20 µm) and clay (<2 µm). If calcite was present, this was removed before handling using an acetic acid-acetate buffer at pH 5 until an aliquot showed no reaction with 10% hydrochloric acid. Organic matter was removed from the clay fractions in the two uppermost horizons using sodium peroxodisulfate (Meier and Menegatti 1997). Powder X-ray diffractograms of the clay fraction were obtained and analysed according to the procedure described by Ernstsen (1998).

Thin sections were prepared from polyester resin impregnated undisturbed soil-samples according to Dalsgaard *et al.* (1981) and Murphy (1986). Thin sections were examined with a petrological microscope (Carl Zeiss Jena – Jenapol) and described according to Bullock *et al.* (1985). Selected thin sections were examined in a Phillips XL40 scanning electron microscope with an energy dispersive X-ray analyser (Norran Voyager 2.7) (SEM-EDX).

Results

Macromorphological Observations

The Flakkebjerg profile consists of three lithologic units and includes the following diagnostic horizons (Table 1): An ochric epipedon (0-26 cm), an agric horizon (26-37 cm) and an argillic horizon (37-100 cm) (Fig. 1 and Table 1). Redoximorphic features were observed from a depth of 37 to 400 cm. The profile was classified as a Typic Agrudalf, fine loamy, mixed, mesic (Soil Survey Staff 1994). The soil structure of the horizons from a depth of 100 cm and deeper were mainly massive, but the second lithologic unit had inclusions of stratified sandy and clayey meltwater-deposits. All three units had macropores of glacial and post-glacial origin. The dominating macropores to a depth of 132 cm were vertical biopores and desiccation fractures. In the second (132-220 cm), and in the top of the third unit (220-260 cm) horizontal shear fractures were identified. In the third lithologic unit (220 cm and downwards) fractures interpreted as due to stress-relief dominated. Pseudogley features were pronounced in the proximity of fractures from 60 cm to about 220 cm (low-chroma depletion hypocoatings adjacent to high-chroma quasi-coatings). The pseudogley features were most pronounced in a few large fractures. The fractures in the third lithologic unit had the opposite pattern with fracture walls covered by intense high-chroma external hypocoatings.

337

Table 1 – Description of the Flakkebjerg-profile.

Horizon	Depth cm	Description
Ap	0-26	Brown (7.5YR 4/2, moist); medium granular structure; many vughs, few channels, common earthworm channels.
EB	26-37	Olive yellow (2.5Y 6/6, moist); common yellowish red mottles (5YR 5/6, moist) and many brown mottles (10YR 5/3, moist); medium to coarse blocky structure; many vughs, vertical planes, channels, and earthworm channels.
Btg1	37-58	Light yellowish brown (2.5Y 6/4, moist); common yellowish brown mottles (10YR 5/4, moist) (ped-surfaces), many clear strong brown (7.5YR 5/6, moist) mottles; medium blocky structure; many vughs, vertical planes and channels, and vertical earthworm channels, few vertical fault-related and desiccation fractures; dominant clay and organic matter coatings (ped-surfaces and earthworm channels); common hypo- and quasi- coatings (fracture walls and ped-surfaces).
Btg2	58-100	Mixture of strong brown (7.5YR 5/6, moist) and light yellowish brown (2.5Y 6/3, moist); medium to coarse blocky structure; common vughs, very few planes, common vertical channels, few vertical earthworm channels, common vertical fault-related and desiccation fractures; dominant coatings consisting of clay minerals (ped-surfaces); common hypo- and quasi-coatings (fracture walls and ped-surfaces).
CBg	100-132	Mixture of strong brown (7.5YR 5/6, moist) and light yellowish brown (2.5Y 6/3, moist); massive structureless; interstitials, very few planes, very few channels, few vertical earthworm channels, common vertical fault-related and desiccation fractures; many hypo- and quasi-coatings (fracture walls).
2Cg1	132-190	Yellowish brown (10YR 5/6, moist) with layers consisting of light yellowish brown (2.5Y 6/3, moist) sandy material; massive structureless; interstitials, many horizontal shear and vertical fault-related fractures; many hypo- and quasi-coatings (fracture walls).
2Cg2	190-220	Same as 2Cg1, but strongly calcareous.
3Cg1	220-400	Gray (5Y 5/1, moist); massive structureless; interstitials, common horizontal shear and vertical relief and fault-related fractures; dominant yellowish red external hypocoatings on fracture walls, common manganese nodules in relation to fracture walls; strongly calcareous.
3Cg2	400-	Same as 3Cg1 but dark gray (5Y 4/1, moist).

338

Table 2 – Horizon data of the Flakkebjerg-profile.

| Horizon | Depth | Particlesize distribution | | | CaCO$_3$ | Organic C | pH$_{CaCl2}$ | Fe$_o^1$ | Al$_o$ | Fe$_d^2$ | Al$_d$ | Fe$_o$/Fe$_d$ |
| | | Clay | Silt | Sand | | | | | | | | |
	cm	g kg^{-1}	g kg^{-1}	g kg^{-1}	g kg^{-1}	g kg^{-1}		g kg^{-1}	g kg^{-1}	g kg^{-1}	g kg^{-1}	
Ap	0-26	136	198	666	0	11.3	5.87	2.5	0.6	6.7	0.9	0.37
EB	26-37	203	221	576	0	2.9	6.22	2.1	0.7	9.2	1.1	0.23
Btg1	37-58	248	356	396	0	1.9	6.47	2.4	0.9	11.2	1.4	0.21
Btg2	58-100	232	270	498	0	1.0	6.57	2.1	0.7	10.1	1.2	0.21
CBg	100-132	189	156	655	0	0.6	6.64	1.6	0.5	8.0	0.9	0.20
2Cg1	132-190	188	139	673	0	0.6	7.24	0.9	0.4	7.4	0.8	0.12
2Cg2	190-220	150	192	658	150	ND^3	7.93	0.4	0.2	4.3	0.3	0.09

Table 3 – Macropore data from the Flakkebjerg-profile.

| Sample | Sampling Depth | Particlesize distribution | | | CaCO$_3$ | Organic C | Fe$_o^1$ | Al$_o$ | Fe$_d^2$ | Al$_d$ | P$_d$ | P$_d$/(Fe$_d$+Al$_d$) |
| | | Clay | Silt | Sand | | | | | | | | |
	cm	g kg^{-1}	g kg^{-1}	g kg^{-1}	g kg^{-1}	g kg^{-1}	g kg^{-1}	g kg^{-1}	g kg^{-1}	g kg^{-1}	mg kg^{-1}	%
Fracture 1	80-100											
hypocoating		170	180	650	0	0.80	0.4	0.4	2.5	1.0	64.5	1.8
quasi-coating		ND^3	ND	ND	0	1.25	2.1	0.4	15.7	1.4	117.5	6.9
Fracture 2	165-175											
hypocoating		160	140	700	0	0.74	0.5	0.4	2.8	0.8	179.5	5.0
quasi-coating		ND	ND	ND	0	0.60	0.9	0.5	5.7	0.8	138.0	2.1
Fracture 3	180-190											
hypocoating		140	140	720	0	1.26	0.4	0.4	2.0	0.7	141.0	5.2
quasi-coating		ND	ND	ND	0	0.77	1.0	0.4	9.9	1.1	118.0	1.0

1. o = Oxalate extractable.
2. d = Dithionite-citrate-bicarbonate extractable.
3. ND = Not determined.

339

Chemical, Physical, and Mineralogical Properties
Horizon Data

The argillic horizon has a relative clay enrichment of approximately 25% (Table 2). Calcite was only found in the 2Cg2 horizon (150 g kg^{-1}). Organic C contents were high only in the Ap horizon (1.1%), but small amounts (0.06%) were found down to 190 cm. The highest ratio of Fe$_o$ to Fe$_d$ (0.37) was observed in the Ap horizon, which is the horizon with the most intense weathering. The largest amounts of Al$_d$ and Fe$_d$ (1.4 and 11.2 g kg^{-1}) occurred in the argillic horizon.

The following clay minerals were identified in the Flakkebjerg profile (Table 3): Kaolinite, vermiculite, HIV (hydroxy interlayered vermiculite), illite, irregularly interstratified illite-smectite, and smectite. Smectite was the dominant clay mineral making up 40-65% of the clay minerals – except in the 2Cg1-horizon, where the content was 5%.
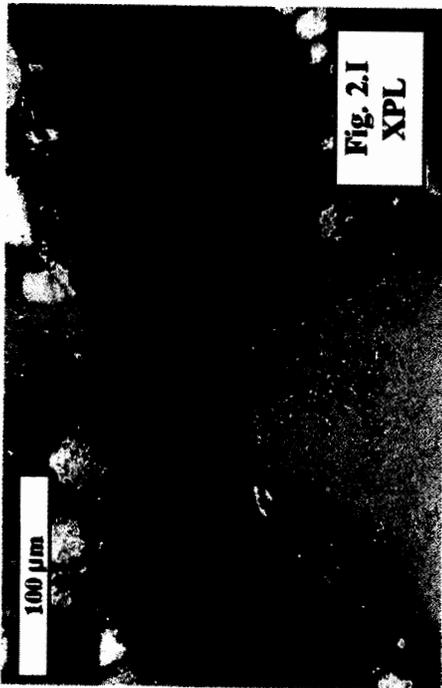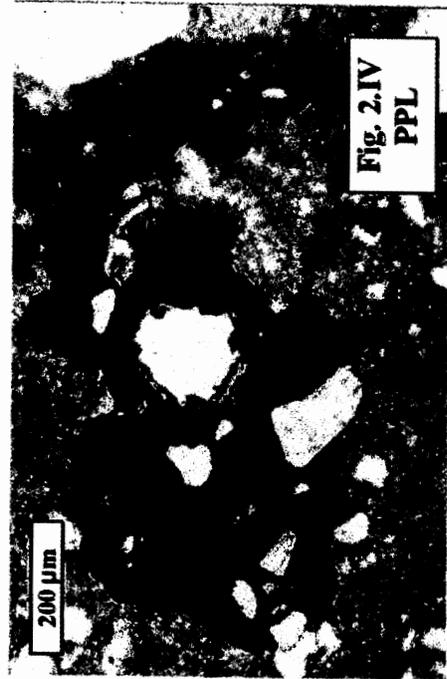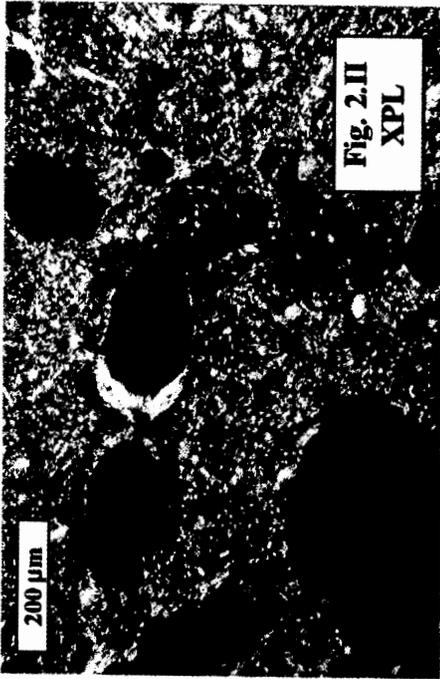
Macropore Data

The particle-size distribution in the hypocoatings of the fractures deviated from the particle-size distribution of the horizons (Table 3), *e.g.* in fracture 1, the clay and silt contents were lower compared to the Btg2 horizon. In fracture 1, the amount of organic C was higher in the quasi-coating (1.25 g kg^{-1}) than in the hypocoating, whereas in fractures 2 and 3 the amount was higher in the hypocoating (0.74 and 1.26 g kg^{-1}).

The contents of oxalate- and dithionite-extractable Al did not indicate marked differences between the hypo- and quasi-coatings, in contrast to the Fe$_o$ and Fe$_d$, which exhibited marked variations, most notable in fracture 1. This fracture had more than 5 times as much Fe$_o$ and more than 6 times as much Fe$_d$ in the quasi-coatings compared to the hypocoatings. In fractures 2 and 3, the quasi-coatings also contained more Fe$_o$ and Fe$_d$ than the hypocoatings. The amounts of P$_d$ represent contents of P within the Fe- and Al-(oxide)hydroxides. Large amounts of P$_d$ were observed in all the coatings (66-180 mg kg^{-1}). In fracture 1, the distribution of P$_d$ followed the sum of Fe$_d$+Al$_d$. In fractures 2 and 3, P$_d$ tended to be higher in the hypocoatings than in the quasi-coatings. The ratio P$_d$/(Fe$_d$+Al$_d$) clearly indicated that the material from the hypocoatings was enriched with phosphate compared with the quasi-coatings.

The clay mineralogical data of the macropore hypocoatings indicated differences in composition compared to the matrix material of the surrounding horizons. In all

---

Fig. 2. Micromorphological images of fractures, quasi-coatings, coatings, and hypocoatings (XPL = Cross-polarized light, PPL = Plane-polarized light): I. Typical limpid microlaminated clay coatings in fracture 2; II. Fe-hypo- and quasi coatings around vesicles in a low chroma soil matrix in Btg1; III. Depletion hypocoating next to a desiccation fracture in Btg2; IV. Mn-hypocoating around vesicle with typic limpid microlaminated clay coatings in Btg1.

340

341

of the three fractures, the smectite content was up to several times higher than in the surrounding soil matrix.

Micromorphological Observations in Macropore Environments

Widespread occurrences of laminated clay and silt coatings were discovered in both inter- and intra-aggregate voids even at depths of 200 cm and indicated that pronounced transport of soil particles had occurred (Fig. 2.I).

A variety of pedofeatures arising from redox processes (pseudogley) in the soil environment next to voids and fractures and in the ped interiors commonly occurred in the EB horizon and in deeper horizons. Adjacent to macropores (interaggregate voids and fractures), large depletion hypocoatings (albans) had developed, some to the extent of several cm thick as observed around the fractures analysed (Table 1). The surface of macropores displayed a complicated pattern with clay or silt coatings, in some cases impregnated or coated with Fe- and/or Mn-oxide-hydroxides (small hypo- and quasi-coatings) (Fig. 2.I, 2.II and 2.IV). Well developed (0.5-2 cm) quasi-coatings composed of Fe-(oxide)hydroxides occurred adjacent to the depletion hypocoatings commonly observed in the first and second lithologic units (Fig. 2.III).

Around fine macro-, meso- and some micropores (voids and fractures) and around sand grains, small ((m-scale) discrete well-impregnated Fe- and/or Mn-hypo- and quasi-coatings were observed in the upper two lithologic units. The sharp boundary between the coatings and the surrounding soil matrix is notable (Figs 2.II and 2.IV). Compared with the pedofeatures described above, these pedofeatures impregnated the surfaces of the voids or the nearsurface areas with Fe- and/or Mn-(oxide)hydroxides, instead of depleting the area. In the third lithologic unit, continuous well-developed external Fe/Mn-hypocoatings were observed on the surface of relief and shear fractures. Redox processes had also resulted in a widespread formation of well-developed Mn-nodules and diffuse Fe-mottles in the soil matrix.

Organic coatings composed of earthworm excrement, together with clay and silt coatings were commonly observed in earthworm channels, especially in the agric horizon, but also in other horizons at a depth of 130 cm. In a few channels and voids, thin organic hypocoatings were observed to a depth of 170 cm and represented evidence for a transport of dissolved or colloidal organic matter.

SEM-EDX Analysis of Macropore Environments

As noted in the micromorphological analysis, Mn-oxides have accumulated around voids and impregnated the soil matrix from the Btg1-horizon and below (Fig. 2.IV, 3, 5, and 6). The elemental composition of the hypocoatings was distinctly different from the soil matrix. The content of Mn increased from 0 to about 27 percent (MnO) and the Fe content increased from about 7 to 19 percent (Fe_2O_3).

In relief fractures from the 3Cg1-horizon, 5 to 10 μm thick external Fe- and Mn-hypocoatings were observed (Figs 4, and 6). These coatings resulted in a strongly contrasting composition between the fracture wall and the soil matrix. SEM-EDX
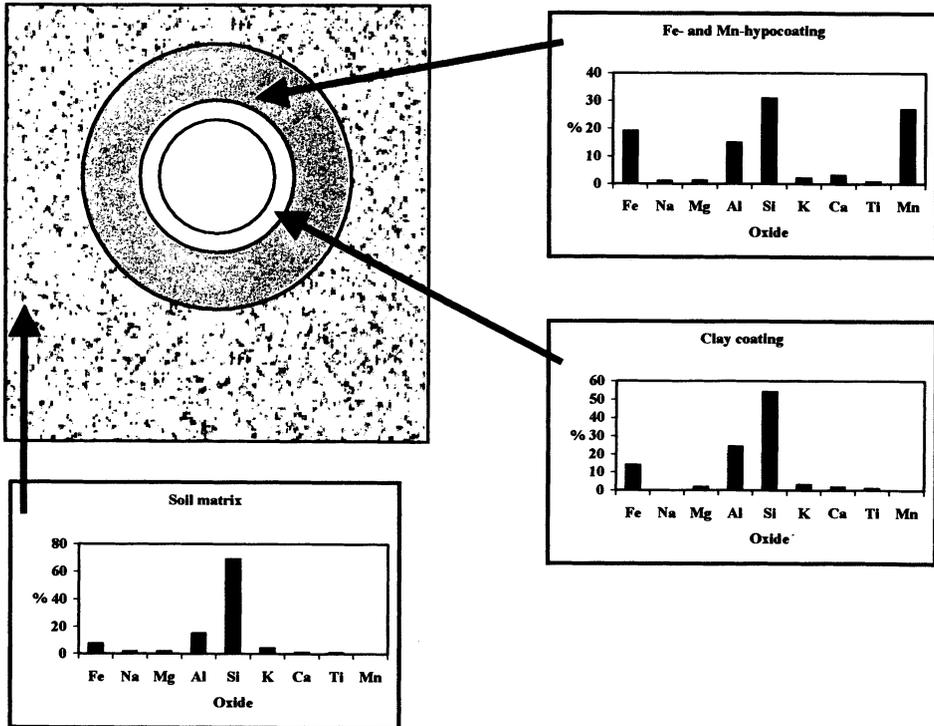
Fig. 3. Semiquantitative composition of coatings in the Btg-horizons as determined by SEM-EDX. The examined coating is the same as shown in Fig. 2.IV and in Fig. 5. Similar coatings were commonly observed in the Btg-horizons. Note the high Mn- and higher Fe-oxide content in the hypocoating.

analysis of this area confirmed that the coatings primarily consist of Mn-oxides with a significant amount of Fe-oxide-hydroxides (Fig. 4).

Discussion

The following discussion will be primarily focused on the contrasting composition of the soil matrix and the soil material around fractures and macropores. Implications with respect to preferential flow patterns will be emphasized.

Contrasting Texture
Lower clay and silt contents were observed in hypocoatings as compared with bulkhorizons. This occurrence may be due to a higher weathering intensity in the fracture zone as compared with the surrounding soil matrix due to ferrolysis
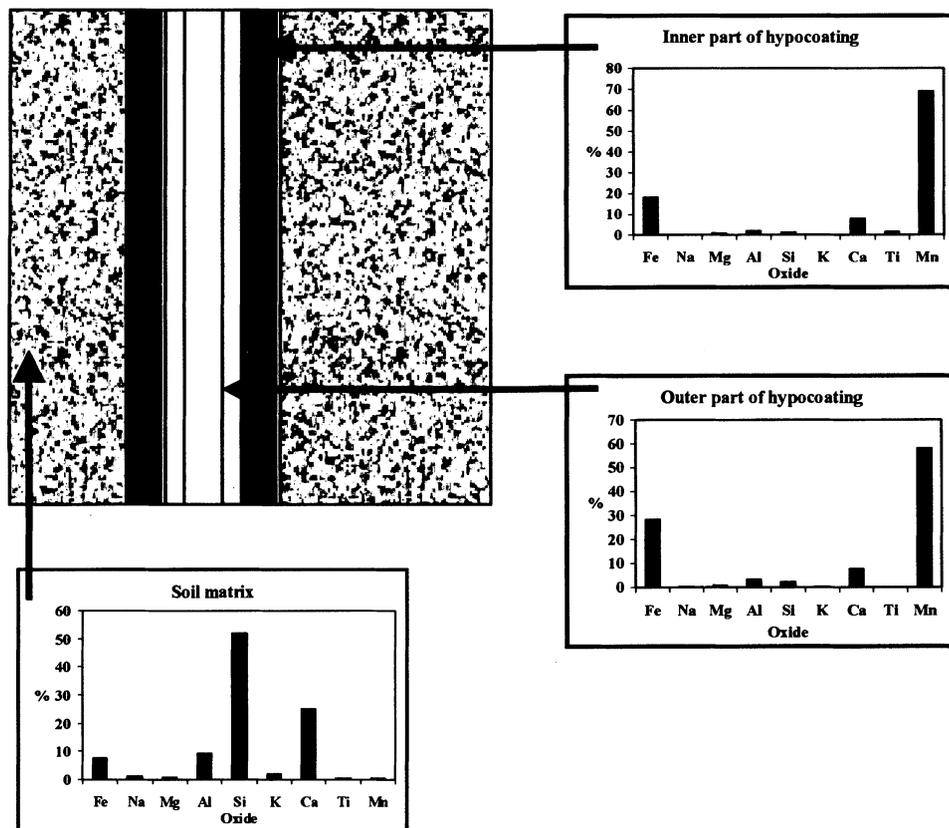
343

Fig. 4. Semiquantitative composition of coatings in the 3Cg-horizons as determined by SEM-EDX. The examined coating is the same as shown in Fig. 6. Similar coatings dominated the fracture walls in the third lithologic unit.

(Brinkman 1970) and/or more intensive eluviation in macropores and fractures. The coarse texture resulted in a higher hydraulic conductivity and a smaller specific surface area in the hypocoating compared to the soil matrix, which indicated a lower sorption capacity in the void wall all other things being equal.

In other macropores clay coatings covered the void walls. The consequence of this phenomenon is a reduction in surface area that can interact with the leaching soil water and a reduced hydraulic conductivity across the void wall that will enhance bypass flow (Sullivan 1994).

Contrasting Clay and Oxide Mineralogy

The clay fraction in all horizons had a rather high content of smectite, in agreement with previous studies (Møberg 1990; Ernstsen 1998). A higher amount of smectite
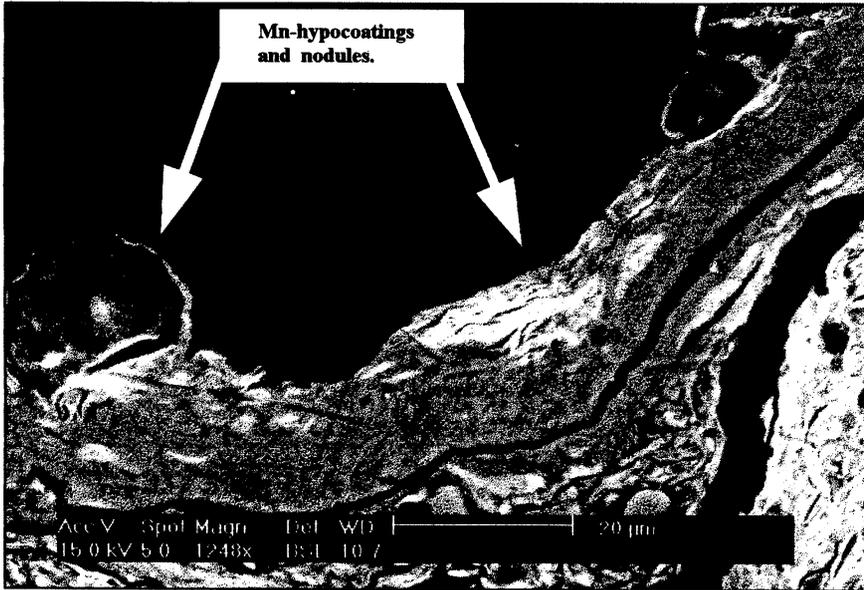
344

Fig. 5. SEM-micrograph of Mn-hypocoating of a void in Btg1. Note the typic limpid clay coatings lining the void wall. The hypocoating is the same as in Fig. 2.IV.
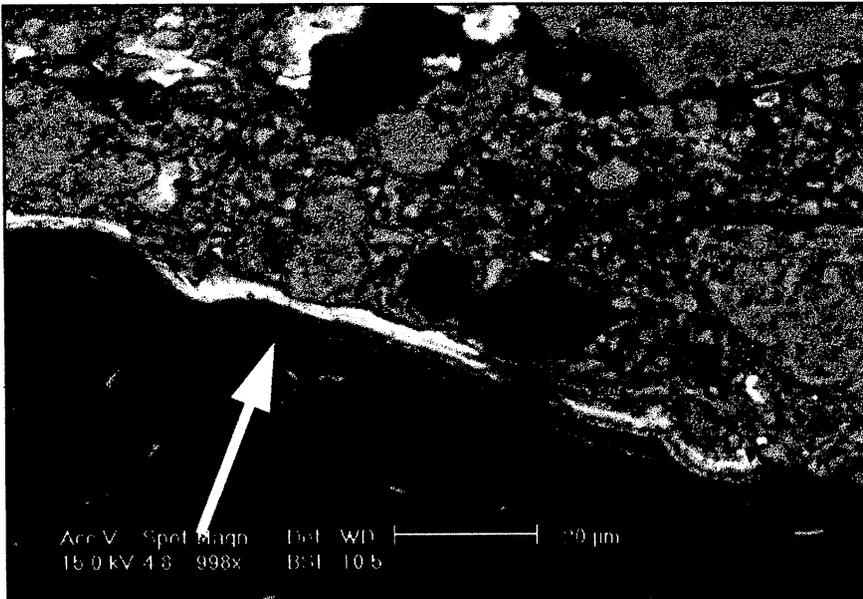

Fig. 6. SEM-micrograph of external anorthic Fe- and Mn-hypocoatings in a relief fracture in 3Cg1. The fracture wall was completely covered with Fe- and Mn-(oxide)hydroxides (arrow).

345

occurred in the hypocoatings as compared to the content in the bulkhorizons.

The occurrence of Fe- and Mn-oxide hypo- and quasi-coatings significantly altered the properties of the void walls of the macropores. Most important was the drastic increase in the ability to specifically sorb anions and heavy metal cations in the quasi-coatings. These coatings also impregnated the microporous soil material adjacent to the voids, thereby decreasing the hydraulic conductivity across macropore walls, and thus enhancing preferential flow patterns (Sullivan 1994).

Contrasting Organic Matter Contents

Enrichment of soil material with organic matter was caused by either root penetration and growth, as observed in fracture 1, or due to deposition of dissolved or particulate humic substances (DPOM) from the near-surface horizons (fractures 2 and 3) (Table 3). The reason for the higher content in the quasi-coatings compared with the hypocoatings in fracture 1 was probably caused by roots penetrating the nutrient-poor hypocoatings in search of plant-nutrients and water. This assertion is supported by the recorded distribution of P_d in Table 4. In fractures 2 and 3, no roots were detected and the distribution of organic C was likely to arise from DPOM, which had been mobilized from the upper soil horizons. In this case, hypocoatings were expected to be the richest in organic C, because the coatings were in close contact with the percolating C-containing soil solution. The content of organic C in the bulk-horizons was less than that in the macropore walls, which is not surprising because roots in fractured clayey till tend to grow in fractures. A higher content of organic matter increases the sorption capacity for hydrophobic compounds due to partitioning (Mallawatantri *et al.* 1996) as well as for some heavy metals (Turner and Steele 1988).

Table 4 – Mineralogical composition of the clay fraction.

Horizon/macropore	HIV[1] %	Kaolinite %	Vermiculite %	Illite %	Illite-smectite %	Smectite %
Ap	8	9	28	5	12	39
EB	6	6	13	7	20	49
Btg1	2	4	16	13	15	51
Btg2	0	7	16	9	18	49
Fracture 1[2]	0	4	10	12	15	59
CBg	0	6	19	11	16	48
2Cg1	2	11	37	21	26	4
Fracture 2[2]	0	5	17	8	16	55
Fracture 3[2]	0	6	34	7	20	34
2Cg2	0	3	11	5	16	65

1. HIV = Hydroxy interlayered vermiculite.
2. The analysed clay fraction was isolated from the depletion hypocoating.
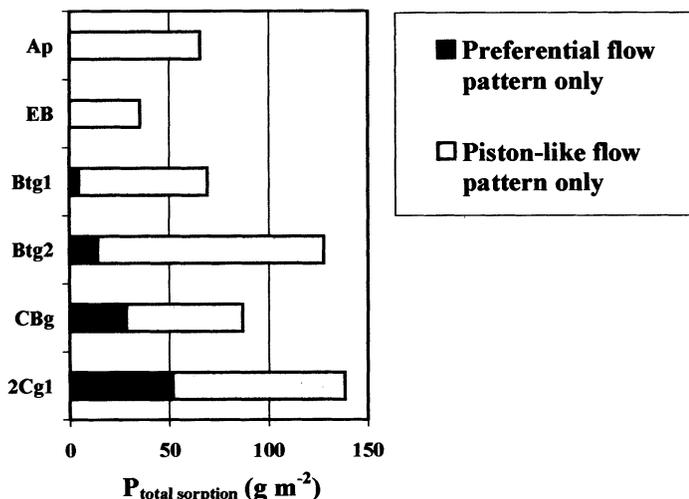
Fig. 7. Predicted phosphate sorption capacities during different flow patterns ($P_{sol.}=10\mu M$).

Implications of Redoximorphic Macropore Environments

The contrasting properties between macropore walls and soil matrix may affect solute sorption, which may be demonstrated using phosphate as a probe for species that are specifically adsorbed. The following equation can be used to estimate the total phosphate sorption capacity of the soil material at threshold concentration of phosphate in solution of 10 μM (Hansen *et al.* 1999)

$$P_{total\ sorption} = 0.0404(Al_0+Fe_0) + 3.5690 \text{(all values in mmol kg}^{-1}) \quad (1)$$

Using this equation, it is seen that the phosphate sorption capacity is lower in the depletion hypocoatings (138-140 mgP kg^{-1}) than in the soil matrix (149-190 mgP kg^{-1}) (see Appendix).

An estimate of the total phosphate sorption capacity of the Flakkebjerg profile can be made based on the following three assumptions:

1. During preferential flow, the phosphate moves in solution from the soil surface through earthworm channels, which have a low affinity for phosphate, and therefore $P_{total\ sorption} = 0$ (Jensen *et al.* 1998).
2. The fraction of soil material that participates in phosphate sorption during preferential transport is equal to the cross sectional area of the profile covered by depletion hypocoatings.
3. In the calcareous 2Cg2 horizon precipitation of Ca-phosphates will hinder further movement of phosphate, and therefore no calculations of $P_{total\ adsorption}$ is made for this horizon.

347

The calculations and the assumptions on which they are based are described in detail in the appendix. As indicated in Fig. 7 the phosphate sorption capacity of the Flakkebjerg soil is around 5 times greater during piston-like matrix flow (99 g m^{-2}) than during preferential flow (523 g m^{-2}). This simple calculation clearly demonstrates the hypothesis that calculations based on bulk horizon properties tend to overestimate the real sorption-properties of a soil profile.

Conclusion

Micropedological investigations revealed marked differences between the soil material adjacent to macropores and the bulk-horizon properties in a Typic Agrudalf. These differences were mainly due to argillization and ongoing redoximorphic processes in the loamy till. The soil material adjacent to the macropores had a lower content of clay and Fe- and Al-(oxide)hydroxides, but a higher content of smectite compared to the soil horizons as a whole. Using phosphate as a probe for species being sorbed, specific calculations indicated that during preferential flow the sorption capacity of the investigated soil was approximately five times less than during piston-like flow. This demonstrates that analysis of soil properties such as sorption and leaching, based on bulk soil analysis may lead to erroneous implications with respect to soil function and quality. Instead, such analysis should be made on that part of the soil, which is actively participating in the soil sorption processes.

Acknowledgements

References

Andreini, M.S., and Steenhuis, T.S. (1990) Preferential paths of flow under conventional and conservation Tillage, *Geoderma, Vol. 46*, pp. 85-102.

Beven, K., and Germann, P. (1982) Macropores and water flow in soils, *Water Res. Research, Vol. 18,* pp. 1311-1325.

Bouyoucos, G.J. (1926) Estimation of the colloidal material in soils, *Science, Vol. 64*, p. 362.

Brinkman, R. (1970) Ferrolysis, a hydromorphic soil forming process, *Geoderma, Vol. 3*, pp. 199-206.

Bullock, P., Fedorof, N., Jongerius, A., Stoops, G., Tursina, T., and Babel, U. (1985) *Handbook for soil thin section description*, Waine Research Publications, Wolverhampton.

Collins, S.H. (1906) Scheibler's apparatus for the determination of carbonic acid in carbonates: An improved construction and use for accurate analysis, *J. Soc. Chem. Industr. (London), Vol. 25*, pp. 518-522.

348

Dalsgaard, K., Baastrup, E., and Bunting, B.T. (1981) The influence of topography on the development of Alfisols on calcareous clayey till in Denmark, *Catena, Vol. 8*, pp. 111-136.

Ernstsen, V. (1998) Clay minerals of clayey subsoils of Weichselian age in the Zealand-Funen area, Denmark, *Bull. Geol. Soc. Denm., Vol. 45*, pp. 39-51.

FAO (1990) *Guidelines for soil profile description*, 3rd edition (revised), Food and Agriculture Organization of the United Nations, Rome.

FitzPatrick, E.A. (1993) *Soil microscopy and micromorphology*, John Wiley & Sons Ltd., Chichester.

Hansen, H.C.B., Jensen, M.B., and Magid, J. (1999) Phosphate sorption to matrix and fracture wall materials in a Glossaqualf, *Geoderma, Vol. 90*, pp. 243-261.

Jardine, P.M., Wilson, G.V., and Luxmore, R.J. (1990) Unsaturated solute transport through a forest soil during rain storm events, *Geoderma, Vol. 46*, pp. 103-118.

Jensen, M.B. (1998) Subsurface transport of phosphorus in relation to its mobilization and immobilization in structured soil, Ph.D.-thesis, The Royal Veterinary and Agricultural University, Copenhagen, Denmark.

Jensen, M.B., Jørgensen, P.R., Hansen, H.C.B., and Nielsen, N.E. (1998) Biopore mediated subsurface transport of dissolved orthophosphate, *J. Environ. Qual., Vol. 27*, pp. 1130-1137.

Jørgensen, P.R., and Fredericia, J. (1992) Migration of nutrients, pesticides, and heavy metals in fractured clayey till, *Géotechnique Vol. 42*, pp. 67-77.

Jørgensen, P.R., Spliid, N.H., Eijsackers, H.J.P., and Hamers, T. (1993) Mechanisms and rates of pesticide leaching in shallow clayey till. pp. 247-251. In: Integrated soil and sediment research: A basis for proper protection: Selected proceedings of the first European conference on integrated research for soil and sediment protection and remediation *(EUROSOL)*, Maastricht, 6-12 September 1992.

Keller, C.K., van der Kamp, G., and Cherry, J.A. (1988) Hydrogeology of two Saskatchewan tills: I. Fractures, bulk permeability and spatial variability of downward flow, *J. Hydr. Neth. Vol. 101*, pp. 97-121.

Khalifa, E.M., and Buol, S.W. (1968). Studies of clay skins in a Cecil (Typic Hapludult) soil: I. Composition and genesis, *Soil Sci. Soc. Am. Proc., Vol 32*, pp. 857-861.

Klint, K.E.S., and Fredericia, J. (1995) Sprækkeparametre i Moræneler (Fracture parameters in Clayey Till), *Vand & Jord, Vol. 2*, pp. 208-214 (in Danish).

Klint, K.E.S., and Gravesen, P. (1999) Fractures and biopores in Weichelian clayey till aquitards at Flakkebjerg, Denmark, *Nordic Hydrology, Vol. 30*, pp. 267-284.

Kronborg, C. (1995) Kvartæret – glaciale aflejringer (Quarternary Glacial Deposits). pp. 271-290. In: Nielsen, O.B. (edt.) *Danmarks geologi fra Kridt til i dag (The Geology of Denmark from the Cretaceous till Holocene)*, Aarhus Geokompendier nr. 1. Geologisk Institut, Aarhus Universitet, Aarhus (in Danish).

Mallawatantri, A.P., McConkey, B.G., and Mulla, D.J. (1996) Characterization of pesticide sorption and degradation in macropore linings and soil horizons of Thatuna silt loam, *J. Environ. Qual., Vol. 25*, pp. 227-235.

McKay, L.D., Cherry, J.A., and Gillham, R.W. (1993) Field experiments in a fractured clay till – 1. Hydraulic conductivity and fracture aperture, *Water Res. Research, Vol. 29*, pp. 1149-1162.

McKay, L.D., and Fredericia, J. (1995) Distribution, origin and hydraulic influence of fractures in a clay-rich glacial deposit, *Can. Geotech. J. Vol. 32*, pp. 957-975.

349

Mehra, O.P., and Jackson, M.L. (1960) Iron oxide removal from soils and clays by a dithion-ite-citrate system buffered with sodium bicarbonate, pp. 317-327. In: Clays and Clay Minerals; Proceedings of 7th International Conference on Clays and Clay Minerals, Washington 1958.

Mehta, N.C., Legg, J.O., Goring, C.A.I., and Black, C.A. (1954) Determination of organic phosphorous in soils: I. Extraction method, *Soil Sci. Soc. Am. Proc., Vol. 18*, pp. 443-449.

Meier, L.P., and Menegatti, A.P. (1997) A new, efficient, one-step method for the removal of organic matter from clay-containing sediments, *Clay Miner., Vol. 32*, pp. 557-563.

Murphy, C.P. (1986) *Thin section preparation of soils and sediments,* A B Academic Publishers, Berkhamsted, Herts.

Møberg, J.P. (1990) Composition and development of the clay fraction in Danish soils. An overview, *Sci. Geol. Bull., Vol. 43*, pp. 193-202.

Nelson, D.W., and Sommers, L.E. (1982) Total carbon, organic carbon, and organic matter. pp. 539-579. In: Page, A.L., Miller, R.H. and Keeney, D.R. (eds.) *Methods of soil analysis. Part 2.* 2nd edition. American Society of Aggronomy and Soil Science Society of America, Madison, Wisconsin.

Schwertmann, U. (1960) Differenzierung der eisenoxide des bodens durch extraktion mit ammoniumoxalate-lösnung, *Z. Pflanzenernärh. Düng. Bodenk., Vol. 105*, pp. 194-202.

Soil Survey Staff (1994) *Keys to soil taxonomy,* 6th edition. U.S. Department af Agriculture, Soil Conservation Service, Pocahontas Press, Blacksburg, Virginia, USA.

Sullivan, L.A. (1994) Structural pore pedofeatures: Influence on some soil properties, pp. 613-622. In: Ringrose-Voase, A.J. and Humphreys, G.S. (eds.): *Soil micromorphology: Studies in management and genesis. Proceedings of the IX international working meeting on soil micromorphology, Townsville, Australia, July 1992.* Developments in soil science 22. Elsevier, Amsterdam-London-New York-Tokyo.

Tiberg, E. (ed.) (1998) Nordic reference soils. 1. Characterisation and classification of 13 typical Nordic soils. 2. Sorption of 2,4 D, atrazine and glyphosate. TemaNord 1998:537. Nordic Council of Ministers, Copenhagen.

Turner, R.R., and Steele, K.F. (1988) Cadmium and manganese sorption by soil macropore linings and fillings, *Soil Sci., Vol. 145*, pp. 79-86.

Vepraskas, M.J., Jongmans, A.G., Hoover, M.T., and Bouma, J. (1991) Hydraulic conductivity of saprolite as determined by channels and porous groundmass, *Soil Sci. Soc. Am. J., Vol. 55*, pp. 932-938.

Vepraskas, M.J., and Wilding, L.P. (1983) Aquic moisture regimes in soils with and without low chroma colors, *Soil Sci. Soc. Am. J., Vol. 47*, pp. 280-285.

Vepraskas, M.J., Wilding, L.P., and Drees, L.R. (1994) Aquic canditions for Soil Taxonomy: concepts, soil morphology and micromorphology, pp. 117-131. In; Ringrose-Voase, A.J. and Humphreys, G.S. (eds.): *Soil micromorphology: Studies in management and genesis,* Proceedings of the IX international working meeting on soil micromorphology, Townsville, Australia, July 1992. Developments in soil science 22. Elsevier, Amsterdam-London-New York-Tokyo.

Vinther, F.P., Eiland, F., Lind, A.M., and Elsgaard, L. (1999) Microbial biomass and numbers of denitrifiers related to macropore channels in agricultural and forest soil, *Soil Biol. Biochem., Vol. 31*, pp. 603-611.

Westergaard, B., and Hansen, H.C.B. (1997) Phosphorus in macropore walls of a Danish Glossudalf, *Acta Agric. Scand., Sect. B, Soil and Plant Sci., Vol. 47*, pp. 193-200.

Appendix

Phosphate sorption capacities of the soil samples were calculated using the equation given in Hansen *et al.* (1999) ($P_{total\ sorption} = 0.0404 \cdot (Al_o + Fe_o) + 3.5690$): Btg2 – 190.2 mg kg^{-1}; 2Cg1 – 149.3 mg kg^{-1}; fracture 1 – 138.1 mg kg^{-1}; fracture 2 – 140.3 mg kg^{-1}; and fracture 3 – 138.1 mg kg^{-1}.

The calculations of the total phosphate sorption capacity of the Flakkebjerg-profile were based on the following assumptions. Bulk densities (ρ_b): Ap – 1,300 kg m^{-3}; EB – 1,700 kg m^{-3}; other horizons – 1,600 kg m^{-3}. Area covered by hypocoatings (HY) were estimated from pointcounting on photographs of the profile and from the profile description: Btg1 – 10%; Btg2 – 15%; CBg – 40%; 2Cg1 – 40%. The $P_{total\ sorption}$ of the hypocoating material was calculated as the mean of $P_{total\ sorption}$ of the investigated fractures (138.8 mg kg^{-1}).

The calculations of the total phosphate sorption capacity of the individual horizons during different flow patterns were performed using the following equations (HT = horizon thickness (m)):

Preferential flow pattern (g m^{-2}):
$$\frac{P_{total\ sorption} \cdot HT \cdot 1\ m^2 \cdot \rho_b \cdot HY}{1000\ mg\ g^{-1} \cdot 1\ m^2}$$

Piston-like flow pattern (g m^{-2}):
$$\frac{P_{total\ sorption} \cdot HT \cdot 1\ m^2 \cdot \rho_b}{1000\ mg\ g^{-1} \cdot 1\ m^2}$$

351

Addresses:
Lars Holm Rasmussen,
Hans Christian Bruun Hansen,
Chemistry Department,
The Royal Veterinary and Agricultural Univ.,
Thorvaldsensvej 40,
DK-1871 Frederiksberg C,
Denmark.

Email: lhr@kvl.dk
       haha@kvl.dk

Vibeke Ernstsen,
Geological Survey of Denmark and Greenland,
Thoravej 8,
DK-2400 Copenhaven NV,
Denmark.

Email: ve@geus.dk